Predicting the peculiar velocities of nearby PSCz galaxies using the Least Action Principle

Article (Published Version)

Mon. Not. R. Astron. Soc. **322**, 121–130 (2001)

Predicting the peculiar velocities of nearby PSC*z* galaxies using the Least Action Principle

J. Sharpe,[1] M. Rowan-Robinson,[1★] A. Canavezes,[1] W. Saunders,[2] E. Branchini,[3] G. Efstathiou,[4] C. Frenk,[3] O. Keeble,[1] R. G. McMahon,[4] S. Maddox,[4] S. J. Oliver,[1] W. Sutherland,[5] H. Tadros[6]† and S. D. M. White[7]

[1]*Astrophysics Group, Blackett Laboratory, Imperial College of Science, Technology and Medicine, Prince Consort Road, London SW7 2BZ*
[2]*Institute for Astronomy, University of Edinburgh, Blackford Hill, Edinburgh EH9 3JS*
[3]*Department of Physics, University of Durham, South Road, Durham DH1 3LE*
[4]*Institute of Astronomy, University of Cambridge, Madingley Road, Cambridge CB3 OHA*
[5]*Department of Physics, University of Oxford, Keble Road, Oxford OX1 3RH*
[6]*Department of Physics, University of Sussex, Falmer, Brighton BN1 9QH*
[7]*Max-Planck-Institut für Astrophysik, Karl-Schwarzschild-Straße 1, 85740 Garching bei München, Germany*

Accepted 2000 September 29. Received 2000 September 29; in original form 1999 January 12

ABSTRACT

We use the Least Action Principle to predict the peculiar velocities of PSC*z* galaxies inside $cz = 2000\,\mathrm{km\,s^{-1}}$. Linear theory is used to account for tidal effects to $cz = 15\,000\,\mathrm{km\,s^{-1}}$, and we iterate galaxy positions to account for redshift distortions. As the Least Action Principle is valid beyond linear theory, we can predict reliable peculiar velocities even for very nearby galaxies (i.e., $cz \leq 500\,\mathrm{km\,s^{-1}}$). These predicted peculiar velocities are then compared with the observed velocities of 12 galaxies with Cepheid distances. The combination of the PSC*z* galaxy survey (with its large sky coverage and uniform selection) with the accurate Cepheid distances makes this comparison relatively free from systematic effects. We find that galaxies are good tracers of the mass, even at small ($\leq 10\,h^{-1}\,\mathrm{Mpc}$) scales; under the assumption of no biasing, $0.25 \leq \beta \leq 0.75$ (at 90 per cent confidence). We use the reliable predicted peculiar velocities to estimate the Hubble constant H_0 from the local volume without 'stepping up' the distance ladder, finding a confidence range of 65–$75\,\mathrm{km\,s^{-1}\,Mpc^{-1}}$ (at 90 per cent confidence).

Key words: methods: numerical – galaxies: distances and redshifts – dark matter – distance scale – large-scale structure of Universe.

1 INTRODUCTION

The relationship between galaxies and matter is one of the most important questions in cosmology. On large scales, there is good evidence that galaxies (and in particular *IRAS* galaxies) are good tracers of the mass. For example, there is the good alignment of the *IRAS* and CMB dipoles (Rowan-Robinson et al. 1990; Strauss et al. 1992), the agreement between predicted peculiar velocities and Tully–Fisher velocities (Willick et al. 1997a), and the consistency of POTENT density fields with density fields from galaxy surveys (Sigad et al. 1998). However, on smaller scales, the reliability of galaxies as tracers of the mass is far from certain.

Investigations of peculiar velocities in the Universe have relied heavily on use of the linear term in gravitational instability theory (e.g. Rowan-Robinson et al. 1990; Strauss et al. 1992; Willick et al. 1997a; da Costa et al. 1998). This has the advantage of being easy and computationally quick, but has the side effect of restricting such analysis to large scales $\sim 10\,h^{-1}\,\mathrm{Mpc}$, where linear theory is valid. In this paper we use the Least Action Principle, which is valid beyond linear theory. It is therefore possible to predict peculiar velocities for nearby galaxies. The Least Action Principle is similar to the more usual action principle, but with the conditions that the initial conjugate momenta are zero and the final positions fixed, instead of the more usual conditions of both the initial and final positions being fixed. It was first used by Peebles (1989, 1990, hereafter P89, P90) to study the dynamics of the Local Group. Later papers (Peebles 1994, 1995) presented different versions of the method, but still dealt mainly with the problem of the Local Group, with only a few external masses. Shaya, Peebles & Tully (1995, hereafter S95) used the method to predict motions for galaxies inside $cz = 3000\,\mathrm{km\,s^{-1}}$, and our methodology is very similar to theirs. Recently, Schmoldt & Saha

★ E-mail: mrr@ic.ac.uk
† Present address: Department of Physics, University of Oxford, Keble Road, Oxford OX1 3RH.

(1998) presented a version of the method directly applicable to redshift space.

Previous work on the local velocity field at small scales has centred mainly on trying to mimic the observed 'cold flow' (low value for the rms of galaxy velocities) of local galaxies in *N*-body simulations (Schlegel et al. 1994; Governato et al. 1997). In both papers it was found to be virtually impossible for an $\Omega_0 = 1$ CDM model to produce a flow as cold of that of the local galaxies. In this paper we will compare the observed peculiar velocities of galaxies with Cepheid distances to their predicted peculiar velocities from the Least Action Principle. This more direct comparison will have the advantage of being less model-dependent. The emphasis of direct comparisons of predicted and observed velocity fields has traditionally been on more distant galaxies. This is due to the wish to use linear theory and the need to have a sufficient number of galaxies to combat the large random errors associated with Tully–Fisher distance measurements. Our analysis is similar to the one by S95, although we restrict our attention to a local sample of galaxies (7/12 of our distances are less than 10 Mpc). We also offer two major improvements. First, the PSC*z* redshift survey has the advantages of greater uniformity and larger sky coverage than the optical catalogue of S95. Secondly, the greater availability of Cepheid distances gives us a far superior (though smaller) set of distances. Both of these improvements should leave our estimate of β and other results freer of systematic errors.

It is difficult to measure H_0 in the local volume, due to the effects of peculiar velocities on the redshifts of galaxies. The traditional approach to this problem has been to extend the distance scale out to distances where the peculiar velocities will be negligible compared to the Hubble flow. However, the reliable peculiar velocities which we predict allow us the possibility of measuring H_0 locally, without 'stepping up' the distance ladder. Such a measurement will obviously be a useful check on more traditional distance ladder determinations.

The layout of this paper is as follows. In the next section we discuss the Least Action Principle. In Section 3 we discuss our mass tracers (mainly the PSC*z* galaxy redshift survey) and the distance estimations we have used. In Section 4 we discuss the results from the peculiar velocity comparison. Finally, in Section 5 we give a discussion of our results.

2 THE LEAST ACTION PRINCIPLE

The action S for a system of point masses in an expanding universe is (P89; P90; S95)

$$S = \int_0^{t_0} \mathrm{d}t L = \int_0^{t_0} \mathrm{d}t \left[\sum_i \frac{m_i a^2 \dot{\boldsymbol{x}}_i^2}{2} - m_i \phi(\boldsymbol{x}_i) \right], \tag{1}$$

where a is the expansion factor for the Universe ($a_0 = 1$), m_i is the mass of the ith particle, $\boldsymbol{x}_i$ is its position, and $\phi(\boldsymbol{x}_i)$ is the gravitational potential.

The action principle is derived by considering changes to the action under infinitesimal changes to the orbits $\boldsymbol{x}_i = \boldsymbol{x}_i + \delta\boldsymbol{x}_i(t)$, and then integrating equation (1) by parts:

$$\delta S = \int_0^{t_0} \delta t \left\{ \sum_i \delta\boldsymbol{x}_i \cdot \left[-\frac{\mathrm{d}}{\mathrm{d}t} m_i a^2 \frac{\delta \boldsymbol{x}_i}{\delta t} + m_i \frac{\delta \phi(\boldsymbol{x}_i)}{\delta \boldsymbol{x}_i} \right] \right\} + \sum_i \left[m_i a^2 \delta\boldsymbol{x}_i \cdot \frac{\mathrm{d}\boldsymbol{x}_i}{\mathrm{d}t} \right]_0^{t_0}. \tag{2}$$

To get the equations of motion from the stationary points of the action, we require the second term to vanish. Normally this is done by setting $\delta\boldsymbol{x}_i = 0$ at the initial and final positions. However, it is also possible to apply the action principle with the boundary conditions $\delta\boldsymbol{x}_i = 0$ at the final position, and $a^2 \delta\boldsymbol{x}_i / \mathrm{d}t = 0$, at the initial position. This condition will be satisfied by the growing mode in linear theory, and it is a natural condition for the early Universe.

We now have to find stationary points of the action. In practice, we will only look for minima. The global minimum will correspond to the solution closest to the Hubble flow, whilst other extrema will apply to solutions where (for example) masses have crossed once and are now falling back into each other. When Peebles (P90) applied the method to the Local Group, only one galaxy (N6822) required a non-minimum solution to be well modelled. To find the minima numerically, we expand the galaxy orbits in terms of a set of trial functions:

$$x_i^\alpha(t) = x_i^\alpha(t_0) + \sum_n C_{i,n}^\alpha f_n(t). \tag{3}$$

Then, to find the orbits, we minimize the action with respect to the coefficients $C_{i,n}^\alpha$. The choice of expansion functions $f_n(t)$ is in theory arbitrary, as long as they satisfy the boundary conditions. However, their growth rate should be consistent with linear theory at early epochs (i.e., $a\,\mathrm{d}x/\mathrm{d}t \rightarrow a^{1/2}$ at $a \rightarrow 0$). We follow previous papers (e.g. P89; P90; S95) in using the set,

$$f_n(t) = (1-a)^n a^{5-n} \left[\frac{5!}{n!(5-n)!} \right], \quad 1 \le n \le 5. \tag{4}$$

The equal spacing of the peaks of these functions allows for good convergence, and their relatively simple form makes them easy to use. The coefficients are found by 'walking down', i.e., by following the gradient of the action towards the minimum. Normally we start with all $C_{i,n}^\alpha = 0$ and iterate according to the equation

$$m_i \delta C_{i,n}^\alpha \propto -\frac{\delta s}{\delta C_{i,n}^\alpha} \tag{5}$$

$$\propto -m_i \int_0^{t_0} \mathrm{d}t \left(a^2 \frac{\mathrm{d}x_i^\alpha}{\mathrm{d}t} \frac{\mathrm{d}f_n}{\mathrm{d}t} + a f_n g_i^\alpha \right), \tag{6}$$

where g_i^α is given by

$$g_i^\alpha = \frac{4}{3}\pi G \rho a x_i^\alpha + \frac{G}{a^2} \Sigma_j m_j \frac{x_j^\alpha - x_i^\alpha}{|\boldsymbol{x}_j - \boldsymbol{x}_i|^3}, \tag{7}$$

and ρ is the mean density of the Universe. This process continues for a sufficient number of iterations (see Section 4.1), so that the $C_{i,n}^\alpha$ have converged to near-constant values. We will then know the orbit of every mass and thus its peculiar motion. We place all of the available mass in the point masses and, unlike previous papers (P90; S95), do not consider the possibility of a smooth component to the mass (which was found to have little effect on the results).

So far our discussion has been in terms of point masses. In reality, though, we will have to apply the Least Action Principle to a set of galaxies. As a result, we will have to make the assumption that all of the mass is concentrated in these galaxies. An important consequence of this assumption is that we require the size of galaxy halo (or group halo; see Section 3.4) to be less than the average distance between galaxies. There is some support for this approximation from studies of the Local Group. Zaritsky et al.

(1989) apply the timing argument to the Milky Way– Leo I system and the Milky Way– M31 system, and find roughly the same mass for the Local Group. As Leo I is at 200 kpc and M31 is at 700 kpc, this implies that the Milky Way does not have a large halo. In addition, Peebles (1994, 1995) finds that it is possible to construct satisfactory orbits for Local Group satellites and nearby groups with simple compact haloes. Another consequence of the assumption that all of the mass is concentrated in galaxies is to place limits on the distribution of loose mass in the Universe (by loose mass we mean mass which is not in haloes). This is particularly important in CDM models where up to 50 per cent of the mass can be loose in an $\Omega_0 = 1$ universe, and greater proportions for lower density universes (Governato, private communication).

At the scale of the Local Group, Branchini & Calberg (1994) and Dunn & Laflamme (1995) have tested the Least Action Principle in CDM universes. The results from these tests are not totally reliable, as the simulations used had either been rescaled for use on Local Group, or lacked resolution. Both papers found a tendency for the Least Action Principle to underpredict Ω_0. Branchini & Calberg attributed these problems to extended haloes, whereas Dunn & Laflamme thought that the problem was more to do with loose mass. Our analysis is at larger scales, so it is not clear what to expect in CDM models.

The condition that the mass is concentrated at the centre of the mass tracers has no chance of being satisfied at early epochs. The best we can hope for is that the perturbations are roughly spherical and centred on the mass tracers. We are, though, entirely concerned with the velocities of galaxies, and these will be generated mainly at late epochs. Thus the problems with the tracing of the density field at early epochs should not be too serious.

3 MASS TRACERS AND DISTANCES

In this section we discuss the galaxy catalogues to which we apply the Least Action Principle. However, raw galaxy catalogues in the form of a list of galaxy positions, redshifts and flux are not suitable to have the Least Action Principle directly applied to them. For example, the raw redshifts will have a contribution both from the Hubble flow and the peculiar velocity of a galaxy, so will not be the true measure of distance we require. Consequently, this section will include not only a description of the galaxy catalogues we use, but also a description of the processes we apply to the galaxy catalogues to make them suitable for calculations with the Least Action Principle.

For peculiar velocity work, there will be certain desirable properties we will want in a galaxy catalogue. The most important of these is that the catalogue is uniformly selected across the sky, as preferential selection in any region will result in false motions being calculated towards that region. Another important property is that we want the catalogue to cover as great a fraction of the sky as possible. All catalogues will have an 'excluded region' or 'mask' around the Galactic plane. In this region it is impossible to select galaxies reliably. In optically selected surveys this is because of absorption from dust. In infrared-selected surveys it is due to cirrus emission. It will clearly be desirable for this excluded region to be as small as possible. The last desirable property is simple density of sampling. The more galaxies we have in a given volume, the greater is the chance we will have of calculating accurate peculiar velocities, assuming that our galaxies are reliable tracers of the mass.

In Section 3.1 we discuss how galaxy bias affects our analysis. We then describe the PSCz survey, our main source of galaxies. Section 3.2 is a general introduction to the catalogue, and is followed by sections on the masked regions, the grouping of galaxies, the Virgo cluster, tidal effects and redshift distortions. In Section 3.8 we discuss how we have treated local galaxies (those with $cz \leq 500\,\mathrm{km\,s^{-1}}$). Finally, in Section 3.9 we present the distance estimations we have used to derive the observed peculiar velocities.

3.1 Galaxy biasing in our analysis

A preliminary issue to be discussed is the effect of bias in the galaxy distribution on our analysis. We need a catalogue of mass tracers on which to apply the Least Action Principle; this will be a catalogue of galaxies and galaxy groups. This means that our analysis will depend on the relationship between the galaxies and the mass. In addition to our requirement that the mass is concentrated in the galaxies (see Section 2), we have uncertainty from whether the mass associated with galaxies is dependent on their environment. This is the problem of the bias of the galaxy distribution. The standard approach to this problem is to use the linear bias factor b to quantify the uncertainty in this relationship (b is given by $\delta_\mathrm{g} = b\delta_\mathrm{m}$, where δ_m and δ_g are the over- or under-densities in the mass and the galaxies respectively). This has the advantage that in linear theory the effect of b is degenerate with that of Ω_0, and the results depend only on $\beta = \Omega_0^{0.6}/b$. However, the Least Action Principle does not rely on linear theory, and one of the main reasons for using it is to probe small scales at which linear theory is invalid. Thus we can no longer expect Ω_0 and b to be fully degenerate. We chose to weight our galaxies on the assumption that there is no bias (i.e., $b = 1$). This is not as restrictive as it might appear. Although strictly Ω_0 and b are not degenerate, we expect that even at non-linear scales a large degeneracy will persist. Support for this comes from Dekel et al. (1993), who investigated the peculiar velocity field using the POTENT methodology. This methodology included non-linear effects, and could in principle break the degeneracy between Ω_0 and b. They found, however, that the individual constraints on Ω_0 and b were extremely weak, and only the parameter β was constrained to good accuracy.

The POTENT analysis is at fairly large scales, with the galaxy and velocity fields being smoothed on $1200\,\mathrm{km\,s^{-1}}$. Our analysis is at smaller scales, and is thus more likely to see the degeneracy between Ω_0 and b broken. Consequently, we have investigated the effect of bias in our calculations. We can do this by modifying the expression used for the potential in equation (1). Including bias, the potential can be expressed as

$$\phi(x) = \left(\frac{\rho_\mathrm{mb}}{\rho_\mathrm{b}}\right)\frac{-Ga^2}{b}\int \mathrm{d}^3x' \frac{\rho(x') - \rho_\mathrm{b}}{|x' - x|}, \tag{8}$$

where $\rho(x')$ is the density of galaxies at x', and ρ_b is the background density of galaxies. ρ_mb is the background density of matter, and the factor $(\rho_\mathrm{mb}/\rho_\mathrm{g})$ just introduces a physical mass (as opposed to galaxy number) into the equation. For $b = 1$, this reduces to the standard form for the potential (Peebles 1980). Using equation (8) for the potential, equation (7) becomes

$$g_i^\alpha = \frac{4}{3}\pi G\rho a x_i^\alpha + \frac{G}{ba^2}\Sigma_j m_j \frac{x_j^\alpha - x_i^\alpha}{|x_j - x_i|^3}. \tag{9}$$

We can then use equation (9) in equation (6) to find the minima of

the action for a biased galaxy distribution and thus investigate the effect of bias. We should note, though, that our treatment is not entirely satisfactory. We have introduced bias in equation (8) in a manner that is reliant on smooth and continuous density fields. However, the Least Action Principle applies to a set of point masses, not continuous fields. We have thus introduced bias in an inconsistent manner. To have introduced bias consistently would have required us to weight galaxies according local density. Such a process would be both complicated and noisy, and so we have chosen not to pursue it. We can, however, expect an investigation of bias using equations (8) and (9) to give at least an indication of its effect on our results.

We therefore did a series of runs with one of our input catalogues with different Ω_0 and b, but constant β (the catalogue we used had a PSCz local weighting and a cloned mask see Sections 3.2–3.8). We then compared the magnitudes of the predicted velocities in the different calculations. For $\beta = 0.5$ ($\Omega_0 = 0.3$, $b = 1$), reducing b to 0.5 ($\Omega_0 = 0.1$) resulted in the velocities decreasing on average by a factor of 0.77 from the $b = 1$ velocities, whilst increasing b to 2 increased the velocities to a factor of 1.29 from the $b = 1$ velocities. Given these results, it is clear that we still have a large degeneracy between Ω_0 and b, and the correct quantity for us to estimate is β. Indeed, with the fairly weak limits we will eventually obtain on β (see Section 4.3) it would be futile to attempt to estimate Ω_0 and b independently. Thus we will only estimate β, and not Ω_0 and b. We will, however, quote our initial results in terms of Ω_0, as we do not wish to hide the assumption that $b = 1$, used in obtaining these results.

An additional consideration comes from the possibility of non-linear bias. If non-linear terms are present in the biasing relation, then they are predicted to be more important at smaller scales (Mo & White 1996) and so could potentially be important for our work. However, most non-linear biasing models tend to differ substantially from linear bias only in clusters or voids (see the models of Mann, Peacock & Heavens 1998). The local volume is neither of these (Kraan-Korteweg & Tammann 1979), so for our analysis most non-linear biasing schemes will be consistent with linear bias and our weighting scheme. As a result, our conclusions on how galaxies trace the mass will be for a general trend and not a particular biasing scheme.

3.2 The PSCz survey

The galaxy catalogue we use is the PSCz survey (Saunders et al. 2000). This is a redshift survey to the full depth ($S_{60} \geq 0.6$ Jy) of the *IRAS* Point Source Catalogue. It has all the properties required for accurate calculation of peculiar velocities. Selection from the *IRAS* Point Source Catalogue ensures near-uniform selection across the sky. In particular, it avoids the problems with optically selected surveys of matching the northern and southern skies. The PSCz survey also has excellent sky coverage, with 84.1 per cent of the sky in the survey. The flux limit of 0.6 Jy makes the PSCz the deepest complete all-sky *IRAS* redshift survey, ensuring that we have sufficient density of sampling to calculate peculiar velocities accurately.

The Least Action Principle is computationally expensive to apply, so we use only galaxies with $cz \leq 2000\,\mathrm{km\,s^{-1}}$ (unless otherwise stated, all of our redshifts have been transformed to the Local Group frame using the Yahil, Tammann & Sandage 1977 correction). For an H_0 of $80\,\mathrm{km\,s^{-1}\,Mpc^{-1}}$, our furthest distance of 17.8 Mpc corresponds to $cz = 1420\,\mathrm{km\,s^{-1}}$, so we have a reasonable buffer zone to the edge effects at $cz = 2000\,\mathrm{km\,s^{-1}}$. Galaxies with $cz \leq 500\,\mathrm{km\,s^{-1}}$, or within 12° of M87 (i.e., in the Virgo cluster) are treated separately (see Sections 3.8 and 3.5 respectively). We impose a luminosity cut, to avoid any weighting problems with the poorly determined faint end of the luminosity function. The luminosity cut is such that all galaxies would have a flux of 0.6 Jy or greater when placed at $cz = 1060\,\mathrm{km\,s^{-1}}$. We give each galaxy a weight $w(cz) = 1/\phi(cz)$, where $\phi(cz)$ is the PSCz selection function (Saunders et al., in preparation). The selection function quantifies the loss of galaxies with distance due to the flux cut. Its value is the number density of galaxies that would be observed at a given redshift in the absence of galaxy fluctuations. The number of galaxies in this main sample is 929. This includes galaxies below the luminosity limit, as these may become sufficiently luminous when we iterate the positions to account for redshift distortions (see Section 3.7).

3.3 Treatment of masked region

Although the PSCz mask is small, we still have to account for it. We do this by filling the sky behind the mask with fictitious galaxies. To test the uncertainties in this, we use two distinct schemes (Rowan-Robinson et al. 2000). The first is the 'random mask', where galaxies are placed at random in the masked region, with a space density consistent with the PSCz selection function. The second is the 'cloned mask' where we extrapolate structures across the Galactic plane from the galaxies we observe above and below the plane. Masked regions away from the Galactic plane (mainly the small areas where *IRAS* did not survey) are still filled with random galaxies. For the random mask we add a total of 169 'galaxies', and for the cloned mask we add 145 'galaxies'.

3.4 Grouping of the galaxies

As we described in Section 2, we are looking for minimum solutions to equation (3), as the global minimum is the solution closest to the Hubble flow. This solution is likely to be adequate, except in regions at the centres of groups and clusters. In these regions, the motions of galaxies are likely to be a general stationary point of the action, as the orbits will have crossed (see P89 and P90). So, to avoid problems with these stationary solutions, we group our galaxies and just follow the motion of the centre of mass. The grouping of galaxies also helps us to deal with redshift distortions. We attempt to iterate out the coherent component to the redshift distortions during our calculations (see Section 3.7). However, there is nothing we can do about the incoherent component to redshift distortions generated on small scales. By grouping the galaxies, we can hope to average out the worst effects of these incoherent redshift distortions. To group galaxies, we use a 'Friends of Friends' algorithm, similar to Huchra & Geller (1982). The linking is $\Delta d = 0.6\,h^{-1}$ Mpc tangentially, and $\Delta z = 150\,\mathrm{km\,s^{-1}}$ radially, for galaxies with average redshift inside $cz = 1060\,\mathrm{km\,s^{-1}}$. For galaxies outside the volume-limited sample we scale the lengths, to allow for the decreasing density of selected galaxies. This is done according to

$$\Delta d = 0.6 \left[\frac{\phi(1060)}{\phi(cz)}\right]^{\frac{1}{3}} h^{-1}\,\mathrm{Mpc}, \tag{10}$$

$$\Delta z = 150 \left[\frac{\phi(1060)}{\phi(cz)}\right]^{\frac{1}{3}} \mathrm{km\,s^{-1}}. \tag{11}$$

The radial linking is so much greater to allow for the effects of

velocity dispersion inside the groups. Once a galaxy is assigned to a group, it is considered to be at the centre of mass of that group. We have compared the groups with those of the Tully (1987) catalogue. Most of the time the two lists of groups agree fairly well, though there were some differences; we are confident that the grouping is working well.

3.5 The Virgo cluster

The Virgo cluster is the most important object for the dynamics of the local volume, so it is important to treat it well in our calculations. To do this, we have treated it separately from the rest of the galaxies. This is necessitated by the large size and velocity dispersion of the cluster. The linking lengths of the grouping algorithm have been chosen for small to medium groups, and are thus inappropriate for the Virgo cluster. We also need to take account of blueshifted galaxies which, outside of the Local Group, are present only in the Virgo cluster. We consider all galaxies with $cz < 2000\,\mathrm{km\,s^{-1}}$ and within 12° of the Virgo core (which we take to be M87) to belong to the Virgo cluster. We cannot extend the upper redshift limit beyond $cz = 2000\,\mathrm{km\,s^{-1}}$ due to contamination from background galaxies. On these criteria, 105 galaxies are placed in the Virgo cluster, which we place at the angular position of M87. For its redshift we use the value given by Bingelli, Tammann & Sandage (1987), not including the dwarf galaxies.

3.6 Tidal effects

Galaxies beyond $cz = 2000\,\mathrm{km\,s^{-1}}$ could potentially generate large tidal motions. We thus calculate these tidal motions using linear theory, and add them to the Least Action Principle results. We use the standard equation,

$$\boldsymbol{V} = \frac{H_0\beta}{4\pi}\Sigma_i w_i \frac{\boldsymbol{r}_i}{r^3}, \tag{12}$$

where w_i is the weight of the ith galaxy (see Section 3.2). The tidal velocities are calculated with all galaxies between $cz = 2000$ and $15\,000\,\mathrm{km\,s^{-1}}$ in the PSCz. The galaxies are placed in the Local Group frame if they are inside $cz = 3000\,\mathrm{km\,s^{-1}}$, but in the CMB frame if they are outside. We use a random mask model throughout for the tidal effects. The tidal velocities are also added to the peculiar velocities when we compensate for redshift distortions. Clearly, the positions of our galaxies, with just the switch in frames at $cz = 3000\,\mathrm{km\,s^{-1}}$, are very crude. We have compared the tidal velocities calculated using these positions with those obtained using a full reconstruction of real space positions. The results compare very well, with most velocities differing by less than $10\,\mathrm{km\,s^{-1}}$.

3.7 Redshift distortions

The redshifts of the galaxies and groups will suffer from redshift distortions due to their peculiar motions. The simple use of these redshifts as distances would cause large errors. As a result, we attempt to iterate out the effects of redshift distortions in a manner similar to S95. This involves iterating the position of a galaxy/group so that the quantity $1/c(H_0 d + v)$ is equal to the redshift of the galaxy (where d is the distance to the galaxy, and v its radial peculiar velocity relative to the Local Group). The peculiar velocities are calculated using the Least Action Principle (see Section 4.1). We iterate the positions 10 times, and the distance a galaxy is allowed to move is slowly scaled down throughout the 10 iterations. By the last iteration most of the residues are small ($\leq 0.5\,h^{-1}\,\mathrm{Mpc}$ in most cases).

We have proper distances for most of the local galaxies (i.e., those with $cz \leq 500\,\mathrm{km\,s^{-1}}$). So, in order to avoid the vagaries of iterating out the redshift distortions, we place these galaxies, where we can, at our distance estimates. It is very important to place these galaxies at the correct distances since, due to their close proximity, they can potentially have a large effect on the motion of the Local Group. The motion of the Local Group is crucial, as all velocities are measured relative to it. To be consistent, we also place the galaxies for which we have Cepheid distances outside $cz = 500\,\mathrm{km\,s^{-1}}$ at those Cepheid distances. An exception is Virgo, which is allowed to iterate to near its distance, and then placed at its distance. This is to allow the correct iteration of the redshifts of galaxies near the Virgo cluster. Although the grouping is done with the galaxies in the Local Group frame, we then attach galaxies below the luminosity cut to groups, or treat them as massless particles. Then, as we iterate out the redshift distortions, and change the distance to galaxies, we re-assess whether galaxies are above or below the luminosity limit, and act accordingly. This may seem quite a trivial effect, but a substantial number of galaxies do change status, in a very systematic way across the sky.

3.8 Weighting of local galaxies

The galaxies inside $cz = 500\,\mathrm{km\,s^{-1}}$ are treated differently from the rest of the survey. This is partly to reflect our increased knowledge of these galaxies, and partly due to their importance in determining the Local Group's velocity (relative to which all other velocities are observed). We did not apply our grouping algorithm to these galaxies, but instead use the seven groups defined by Kraan-Korteweg & Tammann (1979), but follow the pleading of Schmidt & Boller (1992b) for a subdivision of the B7 group.

We have two distinct ways of assigning weights to these local galaxies. The first is using the PSCz catalogue, each group or galaxy being given a weight according to how many galaxies it contains above the luminosity limit, when placed at its distance for $H_0 = 80\,\mathrm{km\,s^{-1}\,Mpc^{-1}}$. The actual value of H_0 used makes little difference to the weights. If a galaxy has no distance and is not in a group with a distance, we use its redshift. A second weighting is given by optical luminosity. We take the optical luminosity data from the catalogue of local galaxies compiled by Schmidt & Boller (1992a), each galaxy and group is weighted in proportion to its luminosity, and all galaxies and groups with a luminosity above $10^{10}\,\mathrm{L_\odot}$ are included (B7a is just under this limit, but too close to the Local Group to cut). To tie these relative weights into the PSCz weightings used for the rest of the galaxies, we multiply the relative weights by the total weight of PSCz galaxies inside $cz = 500\,\mathrm{km\,s^{-1}}$ for $H_0 = 80\,\mathrm{km\,s^{-1}\,Mpc^{-1}}$. The results of these schemes can be seen in Table 1. The main difference in the two weighting schemes is that while the PSCz weighting tends to be fairly even across the galaxies and groups, the optical weighting tends to favour a few large groups. With the two possible mask compensations and the two possible local weightings, we have four possible catalogues.

We have two main aims in having two weighting schemes. First, we wanted to choose the weighting scheme which optimized the results and, secondly, to see how robust the results are to different weighting schemes. The issue of robustness is important. Although either of these weighting schemes might be on average

Table 1. PSCz and optical weightings for the local galaxies. The total weight in each column is 1.00. The group names refer to those of Kraan-Korteweg & Tammann (1979). We give alternatives names in brackets, normally the brightest galaxy.

Group/galaxy	PSCz weight	Optical weight
Local Group	0.09	0.15
B1(Maffei)	0.06	0.23
B2(M81)	0.15	0.09
B3(M101)	0.09	0.10
B4	0.03	0.02
B5(IC4182)	0.06	0.04
B6(N5128)	0.15	0.17
B7a(N300)	0.03	0.02
B7b(N253)	0.06	0.05
N3621	0.03	0.02
N3115	0.00	0.04
N2903	0.03	0.02
N6946	0.03	0.04
N6503	0.03	0.00
N4605	0.03	0.00
N2683	0.03	0.00
N3593	0.03	0.00
N0625	0.03	0.00
N1313	0.03	0.00

a good tracer of the total mass, we expect that the weight assigned to any one galaxy or group is subject to large errors. We can gauge the possible effects of these errors by looking at the results of the two weighting schemes.

3.9 Distances

We present our distances in Table 2. All the distances are derived from Cepheids and seven of the 12 are inside 10 Mpc, making our analysis sensitive to small scales. All of the galaxies are in the PSCz catalogue. The errors consist of the quoted distance errors given in the references, added in quadrature to a 'projection' error for groups. The projection error accounts for the fact that the galaxy to which we have a distance may not be at the centre of the mass of the group. This error is given by

$$\Delta d = \frac{d}{\sqrt{2}n}\sum_i \Delta\Theta_i, \tag{13}$$

where the $\Delta\Theta_i$ are the angular distances of the galaxies from the centre of mass, n is the number of galaxies in the group, and d is the distance to the group. This error is normally the minor contributor, dominating only for B5, B6 and B7a. It is possible that our distances are affected by systematic errors. The most likely sources are either problems with the calibration due to errors in the distance to the LMC, or errors due to metallicity effects. Problems with the calibration at the LMC will affect all the distances by the same fractional amount. Thus, although it will have direct effect on the estimate of H_0, it will leave the rest of our conclusions unchanged. Significant metallicity effects would have the potential to affect all of our results, but luckily they are thought to be small (Kennicutt et al. 1998).

To allow us to better combat redshift distortions in the local volume, we place the groups B1, B4 and B7b and the galaxy N3115 at non-Cepheid distance measures. To avoid possible systematic errors, these are not used in the peculiar velocity comparison. B1 is placed at 4.2 Mpc, from the K-band surface brightness fluctuations measured by Luppino & Tonry (1993). Graham et al. (1984) places B7b 1 Mpc more distant than B7a, so we place it at 3.1 Mpc. The Tully–Fisher ratios of B4 and B5 from Willick et al. (1997b) led us to place B4 at 3.7 Mpc. N3115 is placed at 10.8 Mpc from the planetary nebula luminosity function determination of Ciardullo, Jacoby & Tonry (1993).

Table 2. Distances to nearby galaxies and groups. The redshifts are in the Local Group frame with the Yahil et al. (1977) correction.

Galaxy and group	Dist Mpc	Error Mpc	Red-shift	Reference
M81 (B2)	3.6	0.45	192	Freedman et al. 1994
M101 (B3)	7.4	0.7	374	Kelson et al. 1996
IC 4182 (B5)	4.7	0.5	385	Saha et al. 1994
N5253 (B6)	4.1	0.55	260	Saha et al. 1995
N300 (B7a)	2.1	0.3	137	Freedman et al. 1992
N3621	6.8	0.6	435	Rawson et al. 1997
N0925 (N1023)	9.3	0.8	807	Silbermann et al. 1996
N3351 (Leo I)	10.8	0.9	625	Graham et al. 1997
N3368 (Leo I)	Average used			Tanvir et al. 1995
N2090	12.3	0.9	753	Phelps et al. 1998
N2541	12.4	0.7	593	Ferrase et al. 1998
N7331	15.1	1.4	1115	Hughes et al. 1998
Virgo	17.8	1.8	960	Freedman et al. 1998

Table 3. The convergence of velocities with number of iterations. The velocities are compared to those obtained with 1000 iterations. The results here are for $\Omega_0 = 0.3$, $H_0 = 70\,\mathrm{km\,s^{-1}\,Mpc^{-1}}$, PSC$z$ local weighting and cloned mask. Results from other models are very similar.

Number of iterations	Accuracy of velocities ($\mathrm{km\,s^{-1}}$) ≤ 5	≤ 10	≤ 20	≤ 50
10	2%	17%	64%	97%
20	1%	10%	66%	99%
50	0%	6%	63%	99%
100	5%	60%	94%	100%
150	60%	92%	98%	100%
250	97%	98%	99%	100%

4 RESULTS

In this section we discuss the results from our velocity comparison. Section 4.1 deals with the exact details of how we apply the Least Action Principle. We then discuss the goodness of fit in Section 4.2, and the confidence limits we obtain on Ω_0 and H_0 in Section 4.3.

4.1 Application of Least Action Principle

As explained in Section 2, we iterate the $C^{\alpha}_{i,n}$ towards minimum using equation (6). A crucial point is how many iterations are required to achieve good convergence. We have approached this problem in a different manner to previous papers (P90; S95), which looked at the changing value of the gradient and stopped calculations when this was sufficiently small. Instead, we compared the velocities predicted after a number of iterations with those obtained after 1000 iterations. Typical results can be seen in Table 3. As the table shows, initial convergence to rough values is very quick, but final convergence takes many iterations,

with velocities only changing by a small amount for each iteration. We thus choose to iterate the $C^{\alpha}_{i,n}$ 250 times, iterating galaxy positions every 10 $C^{\alpha}_{i,n}$ iterations for the first 100 iterations (see Section 3.7). The rough velocities used to iterate the positions are easily adequate, as we only aim to drive the residues to $\leq 50\,\mathrm{km\,s^{-1}}$.

In integrating equation (6), we use 10 time-steps. Comparisons with results calculated with 40 and 100 time-steps suggest that this gives us ~85 per cent of velocities within $20\,\mathrm{km\,s^{-1}}$ and ~98 per cent of velocities within $50\,\mathrm{km\,s^{-1}}$. As convergence is slightly slower for a larger number of time-steps, it is clearly preferable to have (as we do) a small number of time-steps combined with a large number of iterations (the computational time is directly proportional to the number of time-steps multiplied by the number of iterations).

As mentioned in Section 2, the solution we seek is the global minimum. This should give us the galaxy orbits which are closest to the Hubble flow, and is the natural extension of linear theory. The existence of a global minimum is guaranteed, as $S \rightarrow \infty$ as $C^{\alpha}_{i,n} \rightarrow \infty$. However, it is also possible that other local minimum exist. Indeed, trials from large random values of $C^{\alpha}_{i,n}$ reveal that multiple minima exist. As a result approximately 15 per cent of galaxies and groups can have two distinct solutions (by distinct solution we mean a difference in velocities of greater than $50\,\mathrm{km\,s^{-1}}$). Unfortunately, it is impossible to calculate the differences in the value of the action between solutions accurately enough to ascertain which solution corresponds to the global minimum. For pure Hubble flow we would have $C^{\alpha}_{i,n} = 0$, so it seems reasonable that the solution obtained when we iterate from $C^{\alpha}_{i,n} = 0$ is the global minimum. Certainly, the use of this solution has become conventional in Least Action work (cf. S95). Thus it is this solution which we use for the results in Sections 4.2 and 4.3. A particular problem we experience is that the Local Group has two distinct solutions for three of the catalogues. Only for the optical local weighting and random mask catalogue do the trials from large random values of $C^{\alpha}_{i,n}$ fail to reveal a second solution. For the other three catalogues, the two Local Group solutions have the potential to cause great problems, as all velocities are measured relative to the Local Group. We have, by fixing the initial values for $C^{\alpha}_{i,n}$, explored the other Local Group solutions for the three catalogues. The results found with these solutions are consistent with those presented below, with similar confidence limits being obtained. For example, with the PSCz local weighting and cloned mask we obtain limits $0.1 \leq \Omega_0 \leq 0.40$ and $65 \leq H_0 \leq 72.5\,\mathrm{km\,s^{-1}\,Mpc^{-1}}$ with the 'standard' solution, iterating from $C^{\alpha}_{i,n} = 0$, and limits of $0.05 \leq \Omega_0 \leq 0.25$ and $65 \leq H_0 \leq 70\,\mathrm{km\,s^{-1}\,Mpc^{-1}}$ with the 'second' solution.

4.2 Goodness of fit

A qualitative impression of the goodness of fit can be obtained from Fig. 1. This presents scatterplot diagrams of the predicted velocities from the Least Action Principle calculations against the observed velocities from the Cepheid distances. All of the plots show results from calculations with a PSCz local weighting and cloned mask. The error bars are given by $\sigma_{oi} = H_0 \Delta D$, where ΔD is the error in the distance, and σ_{oi} is the resulting error in the observed velocity. For all our results, we have calculated the observed velocity errors using $H_0 = 70\,\mathrm{km\,s^{-1}\,Mpc^{-1}}$; we take no account of errors in the predicted velocities. For all the scatterplots where Ω_0 and H_0 are near the best fit (i.e., around $\Omega_0 = 0.2$, $H_0 = 70\,\mathrm{km\,s^{-1}\,Mpc^{-1}}$, see below), almost all of the points lie on the observed velocity equals predicted velocity line, to within their errors. The only exception is the N1023 group (marked in the bottom left plot); even at best fit this point is a considerable distance from the line. So, with the exception of this galaxy, we are getting a very good fit.

To make our results more quantitative, we performed a reduced χ^2 test,

$$\chi^2 = \frac{1}{N-M} \sum_i \frac{(v_{pi} - v_{oi})^2}{\sigma^2_{oi}}. \tag{14}$$

where v_{pi} is the predicted velocity from the Least Action Principle, v_{oi} is the observed velocity, and σ_{oi} its error. N is the number of data points, and M the number of fitted parameters.

Predicted velocities using the Least Action Principle were obtained on a grid of Ω_0 and H_0 for the four possible input catalogues. In Table 4 we present Ω_0, H_0 and the value of the reduced χ^2 statistic at best fit for the four catalogues. We do this using all the galaxies and excluding the outlier N1023 group.

For the reduced χ^2 test we are performing, the 95 per cent confidence limit is 1.83. Thus the results confirm the impression of the scatterplots that the fit is very good, especially when the N1023 group is discarded. The PSCz local weight is performing better than the optical weight, and by a smaller margin the cloned mask is preferred to the random mask. Importantly, we see that the results are reasonably robust to both local weighting and mask compensation, with the best-fitting Ω_0 and H_0 being relatively close for the four models.

We are not sure why we are having such problems with the N1023 group. It is not in the 15 per cent of galaxies and groups for which trials from large random values of $C^{\alpha}_{i,n}$ reveal multiple solutions, nor is the predicted peculiar velocity strongly affected by the multiple solutions of the Local Group. It lies reasonable close to the Galactic plane, so we could be experiencing problems in how we compensate for the mask. The group is an outlier for both the mask models, but it is possible that both models miss an important structure (i.e., a reasonable compact group) that is essential to predict the velocity of N1023 accurately. Another possibility is a problem with the distance to the group. This seems less likely, as the Cepheid distance agrees well with other measurements of 9.6 Mpc from the surface brightness fluctuation method (Tonry et al. 1997), and 10.1 Mpc from the planetary nebula luminosity function method (Ciardullo, Jacoby & Harris 1991). For the purposes of the next section, where we calculate confidence intervals, we chose to exclude the N1023 group. If either of the problems mentioned above are true, then clearly we are well justified in doing so. However, even if N1023 is a natural outlier, then it is necessary to exclude it. The small number of galaxies that we have are not robust to its effect, and fairer limits are obtained without it.

4.3 Confidence intervals

The velocities that we predict for galaxies and groups depend mainly on the input value of Ω_0. There is also a weak dependence on H_0, as this changes where we place the galaxies with measured distances. The main effect of H_0 in the peculiar velocity comparison is that it changes the observed velocities (given by $v = cz - H_0 d$), not the predicted velocities. Fig. 1 shows the effects of changing Ω_0 and H_0. Changing Ω_0 stretches or compresses the range of predicted velocities; thus for low Ω_0

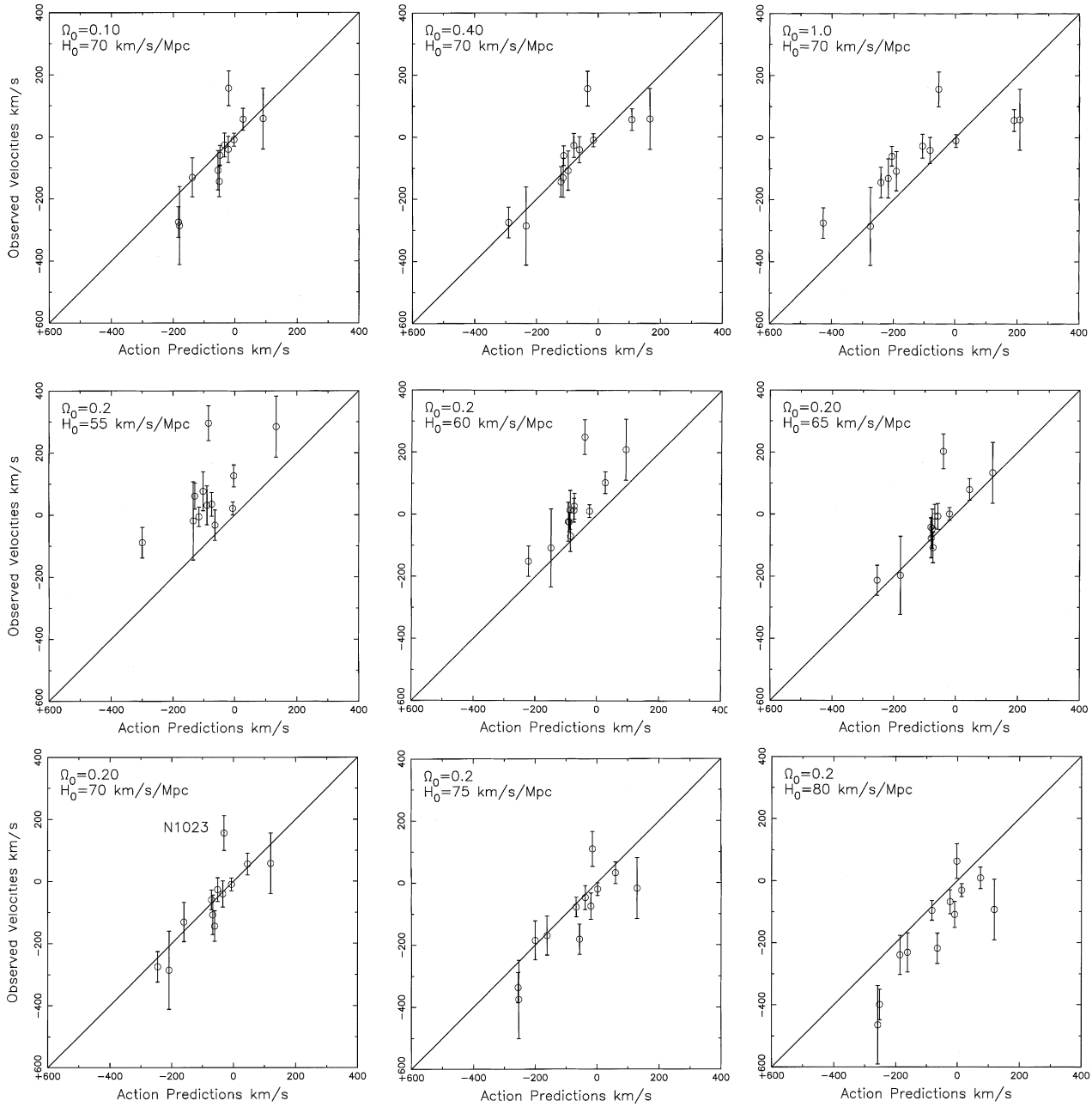

Figure 1. Scatterplots showing the effect of varying H_0 and Ω_0. All results are with PSCz local weighting and a cloned mask model. The line shown is observed velocity = predicted velocity.

Table 4. Best-fitting χ^2 values, with and without N1023. The values of Ω_0 and H_0 given are those at the best-fitting χ^2.

Mask compensation	Local weightings	Full sample χ^2	Ω_0	H_0	Excluding N1023 χ^2	Ω_0	H_0
random	PSCz	1.28	0.40	75	0.64	0.30	70
cloned	PSCz	1.56	0.25	70	0.46	0.25	70
random	optical	2.41	0.25	72.5	1.11	0.20	70
cloned	optical	2.27	0.15	72.5	0.76	0.10	67.5

Table 5. The preferred ranges of Ω_0 and H_0.

Mask compensation	Local weightings	H_0 range km s^{-1} Mpc^{-1}	Ω_0 range
random	PSCz	67.5–75.0	0.10–0.60
cloned	PSCz	65.0–72.5	0.10–0.40
random	optical	65.0–72.5	0.05–0.40
cloned	optical	65.0–72.5	0.05–0.30

our range of predicted velocities is too narrow, whilst for higher Ω_0 it is too broad. Changing H_0 shifts the observed velocities up and down; thus for low H_0 the observed velocities tend to be too large, whilst for high H_0 they tend to be small. In effect, we can think of Ω_0 as changing the gradient of our data, and H_0 as changing the zero-point; only for the certain values of Ω_0 and H_0 will our data be consistent with the observed velocity equals predicted velocity line.

We can make a quantitative assessment of the 90 per cent confidence limits by using a $\Delta\chi^2$ test. The results of this is shown

in Table 5. For all four models, we get similar ranges of Ω_0 and H_0. This indicates that we are robust to the local weighting scheme and to the errors we expect in the weighting given to any individual galaxy or group. We are also reasonable robust to mask compensation model, although the random mask does allow for a higher upper limit on Ω_0. We take our final confidence limits from the union of the results with the PSCz local weighting, as this weighting was preferred. This gives $65 \leq H_0 \leq 75\,\mathrm{km\,s^{-1}\,Mpc^{-1}}$, and $0.1 \leq \Omega_0 \leq 0.60$. We can convert to $\beta = \Omega_0^{0.6}/b$, under the assumption that $b = 1$ (see Section 3.1). This gives us $0.25 \leq \beta \leq 0.75$. Since in the determination of H_0 the distance to Virgo is somewhat controversial, we have calculated an H_0 confidence interval without using this distance for the PSCz local weighting and cloned mask catalogue. We get the same range as before (i.e., $65 \leq H_0 \leq 72.5\,\mathrm{km\,s^{-1}\,Mpc^{-1}}$), so our estimate does not depend very heavily on the distance to Virgo. For interest, we tend to calculate an infall into Virgo of around $200\,\mathrm{km\,s^{-1}}$, for $\beta = 0.5$.

5 DISCUSSION

Using the Least Action Principle and a catalogue of galaxies drawn from the *IRAS* PSCz survey, we have predicted reliable velocities for nearby galaxies. This is consistent with the idea that PSCz galaxies are good tracers of the mass at small as well as large scales. As mentioned in Section 2, we are assuming galaxies are point masses and would not have expected to predict reliable velocities if galaxy haloes where very extended, or the Universe contained a lot of loose matter. Consequently, our ability to predict reliable velocities on scales ranging from 2 to 15 Mpc argues against galaxies having extended haloes beyond 2–3 Mpc. It is also difficult to reconcile large amounts of loose matter with the good fit we observe. A possible solution to this is that the loose matter is distributed fairly evenly so that it produces no net accelerations. Another possibility is that the clustering (above galaxy scale) of the loose matter is tightly correlated with the clustering of galaxies. CDM models contain a lot of loose matter (see Section 2), so the good fit we observe is a challenge for such models. Indeed, as discussed in the introduction, the two previous attempts at testing the Least Action Principle in CDM simulations (Branchini & Calberg 1994; Dunn & Laflamme 1995) were not successful. It would clearly be desirable to repeat these investigations with an increased number of particles and consequently higher resolution. It could then be established whether the Least Action Principle should predict reliable velocities in CDM universes and allow an assessment of the effect on Least Action Principle predictions of galaxy merging, mass transfer and tidal disruption.

If we neglect bias (i.e., assume $b = 1$), then the Ω_0 results confirm the difficulty of fitting the local flow for values of Ω_0 around unity. Governato et al. (1997) found no cases of a CDM simulation with either $\Omega_0 = 0.3$ or $\Omega_0 = 1$, producing a 'cold flow' as low as that observed. Their definition of 'cold flow' was the rms velocity inside $cz = 500\,\mathrm{km\,s^{-1}}$. They used a value of $60\,\mathrm{km\,s^{-1}}$ from Schlegel et al. (1994). The data we use here yield an equivalent 'cold flow' of $43 \pm 35\,\mathrm{km\,s^{-1}}$, so the results are consistent. However, our results have greater model independence, especially with regard to the normalization of the power spectrum.

Direct comparisons of peculiar velocities have been made at larger scales, with the use the of Tully–Fisher distances. Willick et al. (1997a) use the 1.2-Jy galaxy redshift survey and the Mark III catalogue of peculiar velocities to achieve an estimate of $\beta = 0.49 \pm 0.07$. Da Costa et al. (1998) use the 1.2-Jy survey with SFI peculiar velocities to get $\beta = 0.6 \pm 0.1$. The confidence limits we derive of $0.25 \leq \beta \leq 0.75$ are quite consistent with these estimates. For the PSCz local weighting we get a best-fitting Ω_0 of around 0.3, which gives $\beta = 0.5$. This agrees well with the Willick and da Costa estimates, and suggests that there is little variation of the measured β with the scale the estimate is made on. Such a dependence of measured β with scale has been invoked to explain the difference in β estimates between velocity–velocity comparisons (Willick et al. 1997a; da Costa et al. 1998; this paper) and density–density comparisons using the POTENT methodology (Sigad et al. 1998, who estimate $\beta = 0.89 \pm 0.12$). As we find no evidence for such a scale dependence, we suggest that the source of the discrepancy must lie elsewhere. S95 use the Least Action Principle and Tully–Fisher data to estimate $\Omega_0 = 0.17 \pm 0.1$ (giving $\beta = 0.35 \pm 0.15$, for $b = 1$). Again this is consistent with our results, but despite the similarities in methodology, our results are less comparable with this paper, which uses an optical catalogue for its mass tracers.

The classical way to estimate H_0 has been through the distance ladder. Typically this means using Cepheid distances to nearby galaxies, groups and clusters to calibrate either type Ia supernova (SN Ia), or the Tully–Fisher relation. Direct estimates from the Virgo cluster are also made. There tends to be a bifurcation of estimates; for example, Freedman et al. (2000) give a value $H_0 = 72 \pm 3$ (statistical) ± 7 (systematic) $\mathrm{km\,s^{-1}\,Mpc^{-1}}$, whilst Tammann (2000) gives $H_0 = 58 \pm 6\,\mathrm{km\,s^{-1}\,Mpc^{-1}}$. The disagreements causing these different estimates are wide-ranging. Some of the more important are the distance to the Virgo cluster, the nature of the Fornax cluster, suitable SN Ia observations for calibration purposes, the use of the decline rate– absolute magnitude relation for SN Ia, and the magnitude of systematic effects when using the Tully–Fisher relation. We obtain the confidence interval 65–$75\,\mathrm{km\,s^{-1}\,Mpc^{-1}}$, which favours the higher estimate. Importantly, the methodology we have used by passes many of the disagreements, relying mainly on the non-controversial Cepheid distances. Of the disagreements listed above, only the distance to Virgo applies to our estimate, and, as shown in Section 4.3, it is of little importance for our estimate.

Recently, a number of H_0 estimates from the *HST* Key Project have been presented. These Key Project estimates have been made with a variety of secondary distance indicators. These include the surface brightness fluctuations method [$H_0 = 69 \pm 4$ (statistical) ± 5 (systematic) $\mathrm{km\,s^{-1}\,Mpc^{-1}}$; Ferraresa et al. 2000], the Fundamental Plane relation [$H_0 = 78 \pm 7$ (statistical) ± 8 (systematic) $\mathrm{km\,s^{-1}\,Mpc^{-1}}$; Kelson et al. 2000], the Tully–Fisher relation [$H_0 = 71 \pm 4$ (statistical) ± 10 (systematic) $\mathrm{km\,s^{-1}\,Mpc^{-1}}$; Sakai et al. 1999] and the Type Ia SN method [$H_0 = 68 \pm 2$ (statistical) ± 5 (systematic) $\mathrm{km\,s^{-1}\,Mpc^{-1}}$; Gibson et al. 2000]. Perhaps the most interesting of these estimates is the Type Ia SN result (Gibson et al. 1999). This method has traditionally favoured the lower H_0 estimates (e.g. Saha et al. 1997, 1999), and thus this higher estimate removes one of the major objections to a high value for H_0. Our estimate for H_0 (65–$75\,\mathrm{km\,s^{-1}\,Mpc^{-1}}$) agrees very well with these *HST* Key Project determinations. Given that our estimate avoids many of the traditional disagreements in distance ladder determinations, and that the *HST* Key Project aims to provide a definitive estimate of H_0, this amounts to a strong argument for a high H_0.

Although our estimate is made in the local volume, it is not a local estimate of H_0. We use the PSCz selection function to weight the galaxies, so if we live in a local over- or under-density this will

be fully taken into account. As a result, any net expansion or contraction of the local volume will be accounted for in the Least Action Predictions. Thus our estimate of H_0 will in effect be made to at least the average depth of the PSCz ($cz = 8100\,\mathrm{km\,s^{-1}}$), and will be a global, not a local, estimate. We would like to reiterate that, like all estimates of H_0 made with Cepheids, this value is vulnerable to errors from metallicity effects, or more importantly, an error in the distance to the LMC.

ACKNOWLEDGMENTS

JS thanks PPARC for a research studentship. We thank Fabio Governato for useful correspondence, and Robert Mann for thorough readings of drafts of this paper, which led to great improvements. We also thank a referee for helpful comments which led to the paper being improved.

REFERENCES

Bingelli B., Tammann G., Sandage A., 1987, AJ, 94, 251
Branchini E., Calberg R. G., 1994, ApJ, 434, 37
Ciardullo R., Jacoby G. H., Harris W. E., 1991, ApJ, 383, 487
Ciardullo R., Jacoby G. H., Tonry J. L., 1993, ApJ, 419, 479
da Costa L. N., Nusser A., Wolfram F., Giovanelli G., Haynes M. P., Salzer J. J., Wenger G., 1998, MNRAS, 299, 425
Dekel A., Bertschinger E., Yahil A., Strauss M. A., Dacis M., Huchra J. P., 1993, ApJ, 412, 1
Dunn A. M., Laflamme R., 1995, ApJ, 443, L1
Ferrarese L. et al., 2000, ApJ, 507, 655
Ferrarese L. et al., 2000, ApJ, 529, 745
Freedman W. L., Madore B. F., Hawley S. L., Horowitz I. K., Mould J., Navarrete M., Sallmen S., 1992, ApJ, 396, 80
Freedman W. L., et al., 1994, ApJ, 427, 628
Freedman W. L., Mould J. R., Kennicutt R. C., Jr., Madore B. F., 2000, ApJ, in press (astro-ph/0012376)
Gibson B. K. et al., 2000, ApJ, 512, 48
Governato F., Moore B., Cen R., Stadel J., Lake G., Quinn T., 1997, New Astronomy, 2, 91
Graham J. R., 1984, AJ, 89, 1332
Graham J. A. et al., 1997, ApJ, 477, 535
Huchra J. P., Geller M. J., 1982, ApJ, 257, 423
Hughes S. M. G. et al., 1998, ApJ, 501, 32
Kelson D. D. et al., 1996, ApJ, 463, 26
Kelson D. D. et al., 2000, ApJ, 529, 768
Kennicutt R. C., Jr. et al., 1998, ApJ, 498, 181
Kraan-Korteweg R. C., Tammann G. A., 1979, Astron. Nachr., 300, 181
Lupppino G. A., Tonry J. L., 1993, ApJ, 410, 81
Mann R. G., Peacock J. A., Heavens A. F., 1998, MNRAS, 293, 209
Mo H. J., White S. D. M., 1996, MNRAS, 282, 347
Peebles P. J. E., 1980, The Large-Scale Structure of the Universe. Princeton Univ. Press, Princeton
Peebles P. J. E., 1989, ApJ, 344, L53 (P89)
Peebles P. J. E., 1990, ApJ, 362, 1 (P90)
Peebles P. J. E., 1994, ApJ, 429, 43
Peebles P. J. E., 1995, ApJ, 449, 52
Phelps R. L. et al., 1998, ApJ, 500, 763
Rawson D. M. et al., 1997, ApJ, 490, 517
Rowan-Robinson M. et al., 2000, MNRAS, 314, 375
Rowan-Robinson M. et al., 1990, MNRAS, 247, 1
Saha A., Labhardt L., Schwengeler H., Macchetto F. D., Panagia N., Sandage A., Tammann G. A., 1994, ApJ, 425, 14
Saha A., Sandage A., Labhardt L., Schwengeler H., Tammann G. A., Panagia N., Macchetto F. D., 1995, ApJ, 438, 8
Saha A. et al., 1997, ApJ, 486, 1
Saha A. et al., 1999, ApJ, 522, 802
Sakai S. et al., 2000, ApJ, 529, 698
Saunders W. et al., 2000, MNRAS, 317, 55
Schlegel D., Davis M., Summers F., Holtzman J. A., 1994, ApJ, 427, 527
Schmidt K. H., Boller T., 1992a, Astron. Nachr., 313, 189
Schmidt K. H., Boller T., 1992b, Astron. Nachr., 313, 329
Schmoldt I. M., Saha P., 1998, AJ, 115, 2231
Shaya E. J., Peebles P. J. E., Tully R. B., 1995, ApJ, 454, 15 (S95)
Sigad Y., Eldar A., Dekel A., Strauss M. A., Yahil A., 1998, ApJ, 495, 516
Silbermann N. A. et al., 1996, ApJ, 470, 1
Strauss M. A., Yahil A., Davis M., Huchra J. P., Fisher K., 1992, ApJ, 397, 395
Tammann G. A., 1998, preprint (astro-ph/9803255)
Tanvir N. R., Shanks T., Ferguson H. C., Robinson D. R. T., 1995, Nat, 377, 27
Tonry J. L., Blakeslee J. P., Ajhar E. A., Dressler A., 1997, ApJ, 475, 399
Tully R. B., 1987, ApJ, 321, 280
Willick J. A., Strauss M. A., Dekel A., Kolatt T., 1997a, ApJ, 486, 629
Willick J. A., Courteau S., Faber S. M., Burstein D., Dekel A., Strauss M. A., 1997b, ApJS, 109, 333
Yahil A., Tammann G. A., Sandage A., 1977, ApJ, 217, 903
Zaritsky D., Olszewski E. W., Schommer R. A., Peterson R. C., Aaronson M., 1989, ApJ, 345, 759

This paper has been typeset from a TEX/LATEX file prepared by the author.